1 up

X-621-72-107
PREPRINT

NASA TM X- 65900

EFFECT OF MODIFIED THERMAL CONDUCTIVITY ON THE TEMPERATURE DISTRIBUTION IN THE PROTONOSPHERE

H. G. MAYR
ERNEST G. FONTHEIM
K. K. MAHAJAN

APRIL 1972

GODDARD SPACE FLIGHT CENTER
GREENBELT, MARYLAND

EFFECT OF MODIFIED THERMAL CONDUCTIVITY ON THE TEMPERATURE DISTRIBUTION IN THE PROTONOSPHERE

H. G. Mayr, Ernest G. Fontheim, and K. K. Mahajan*

April 1972

Goddard Space Flight Center
Greenbelt, Maryland

*Radio Science Division, National Physical Laboratory, New Delhi-12, India.

EFFECT OF MODIFIED THERMAL CONDUCTIVITY ON THE TEMPERATURE DISTRIBUTION IN THE PROTONOSPHERE

by

H. G. Mayr, Ernest G. Fontheim, and K. K. Mahajan

ABSTRACT

At typical protonospheric electron densities the electron mean free path is sufficiently long so that the coefficient of thermal conductivity is no longer given by Spitzer's expression. The effect on the temperature profile of using the corrected expression for conductivity is investigated. The corrected thermal conduction coefficient is density-dependent and has a more complicated temperature dependence than the coefficient applicable to higher density plasmas. The results indicate that the effect is not negligible even under quiet conditions and at low latitudes.

EFFECT OF MODIFIED THERMAL CONDUCTIVITY ON THE TEMPERATURE DISTRIBUTION IN THE PROTONOSPHERE

Recent daytime temperature measurements by two satellites at different points along the same magnetic field line inside the plasmasphere have allowed us to deduce the field aligned temperature gradients (see Fig. 1). It is, therefore, of interest to investigate whether the presently used value of the heat conduction coefficient is consistent with these data. Recently, Mayr et al. (1972) have solved the simultaneous continuity, momentum, and energy equations for a multi-component ionosphere. Using their model we have investigated the effect of a modified coefficient of heat conduction on the temperature profile. It is well known that the thermal conductivity coefficient for plasmas obtained by Spitzer and Härm (1953) is no longer valid when the mean free path λ approaches the characteristic length ℓ_c given by $(1/T\ dT/ds)^{-1}$ or even becomes larger than ℓ_c. Mayr and Volland (1968) have derived an improved expression for the thermal conductivity in the form of a power series in λ/ℓ_c. These authors define two mean free paths, λ_- referring to particles approaching the point s = 0 from below and λ_+ referring to those approaching from above. s = 0 is the point about which the expansion is taken. It is shown that to second order in λ/ℓ_c the heat conduction flux can be expressed by the following relation:

$$j = -\frac{k}{4}\bar{c}\ (\lambda_+ + \lambda_-)\ n_e \frac{dT}{ds} - \frac{3k}{32}\bar{c}\ (\lambda_+^2 - \lambda_-^2)\ n_e \frac{d^2T}{ds^2} \tag{1}$$

$$\equiv \kappa_{eff}\ T^{5/2}\frac{dT}{ds}. \tag{2}$$

where c is the mean speed of the electrons, n_e the electron density, k is Boltzmann's constant, s the coordinate along the magnetic field line, and the effective conductivity κ_{eff} is defined by Equation (2). The conductivity is now a function of the electron density.

If $\lambda_+ \neq \lambda_-$, then $\lambda_+ - \lambda_- > 0$, because λ_+ refers to a higher altitude than does λ_-. Furthermore, the electron temperature has a maximum in the equatorial plane (under symmetrical conditions), and therefore its second derivative is negative. As a result, the correction term in Equation (1) has the effect of reducing the thermal conductivity, as is to be expected.

The mean free path has the general form

$$\lambda = K \frac{T^2}{n}, \tag{3}$$

where the constant K has been chosen such that κ_{eff} reduces to the conductivity of Spitzer and Härm if $\lambda_+ = \lambda_-$ and the electron distribution is Maxwellian. In that case

$$K \sim 3 \times 10^4 \text{ cgs units.}$$

λ_+ and λ_- in Equation (1) have been calculated from Equation (3) by using the values of T and n at distances $\lambda/2$ above and below the point $s = 0$ respectively.

In order to estimate the range of values of κ_{eff} along the field lines of interest here, the effective conductivity has been calculated for a number of different density profiles and a fixed temperature profile. The results are shown in Figure 2. The curves are labelled by the electron density at 2500 km (equatorial plane). The values of κ_{eff} in the shaded region correspond to realistic density profiles. The straight line represents the conductivity κ_{SH} of Spitzer and Härm (1953) which is density-independent. Hence, it is seen that the correction to κ_{SH} is at most 15% in this particular case.

Figure 3 shows two calculated temperature profiles along the 30° field line (equatorial radius = 2500 km). In addition the Explorer 22 and 32 temperature measurements at 1000 km and 2500 km respectively along the same field line are shown. The rectangular boxes indicate midday ranges of altitude and temperature (see Fig. 1). These profiles have been obtained by solving the continuity, momentum, and energy equation's so that each temperature profile is consistent with the electron density profile used in the energy equation. The lower boundary value of the electron temperature is $T_{eo} = T_n = 1050°K$. Curve (1) was calculated by using the conductivity κ_{SH} and a photoelectron flux at 300 km of 2.5×10^9 cm^{-2} sec^{-1} of 10 ev. The temperature gradient is clearly too small.

If the modified heat flux given by Equations (1) and (2) is used, then one obtains curve (2). κ_{eff} was calculated with the temperature and density values corresponding to curve (1). The same photoelectron flux as in curve (1) was used to obtain the heating rates. The O^+, H^+, and electron density profiles corresponding to curve (2) are shown in Figure 4. These profiles were obtained simultaneously with the temperature profile and are based on an upward H^+ flux in the protonosphere of 2.7×10^7 cm^{-2} sec^{-1}, typical of daytime conditions. This flux value was chosen in order to obtain electron density values in agreement with the measured ones.

The effect of the diminished conductivity is to increase the temperature gradient, as is to be expected. However, the calculated gradient is still smaller than the observed one. It should also be pointed out that this calculation was carried out for a relatively low latitude. Since the corrected thermal conductivity is density-dependent and the density decreases toward higher L-values, it is clear that at higher L-values the effect on the temperature profile due to the corrected conductivity coefficient will be even more pronounced.

ACKNOWLEDGMENT

This work was performed while two of us (EGF and KKM) held NAS-NRC Research Associateships at Goddard Space Flight Center.

REFERENCES

Brace L. H., "The Global Structure of Ionosphere Temperature," Space Research X, T. M. Donahue, P. A. Smith, L. Thomas, ed's. North-Holland Publishing Co., Amsterdam, 1970 (p. 633).

Mayr H. G., Fontheim E. G., Brace L. H., Brinton H. C., Taylor H. A. Jr., "A Theoretical Model of the Ionosphere Dynamics with Interhemispheric Coupling," J. Atm. Terr. Phys. (1972) to be published.

Mayr H. G. and Volland H., "Model of Magnetospheric Temperature Distribution," J. Geophys. Res., 73, 4851 (1968).

Spitzer L. and Härm R., "Transport Phenomena in a Completely Ionized Gas," Phys. Rev. 89, 977 (1953).

LIST OF FIGURES

Figure 1. Combined T_e measurements for Explorers 32 and 22 along a single field tube L = 1.4. The difference in temperature at these two altitudes reflects the temperature gradient along this tube (from Brace, 1970).

Figure 2. Calculated effective heat conductivity for different density profiles.

Figure 3. Calculated temperature profiles for the cases of the conductivities κ_{SH} (curve 1) and κ_{eff} (curve 2).

Figure 4. O^+, H^+, and electron density profiles corresponding to the temperature profile of curve 2 in Figure 3.

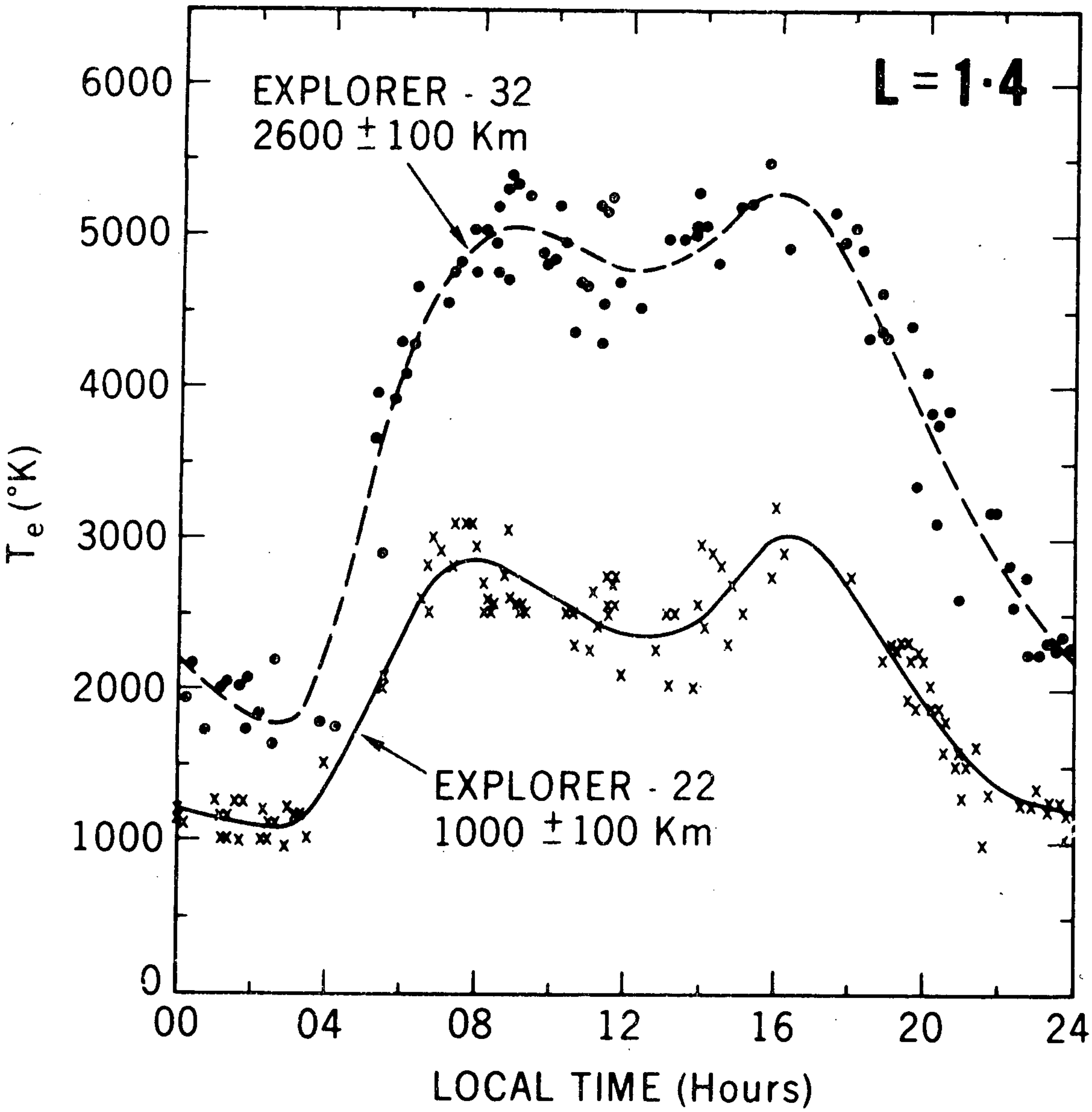

Figure 1. Combined T_e measurements for Explorers 32 and 22 along a single field tube L = 1.4. The difference in temperature at these two altitudes reflect the temperature gradient along this tube (from Brace, 1970).

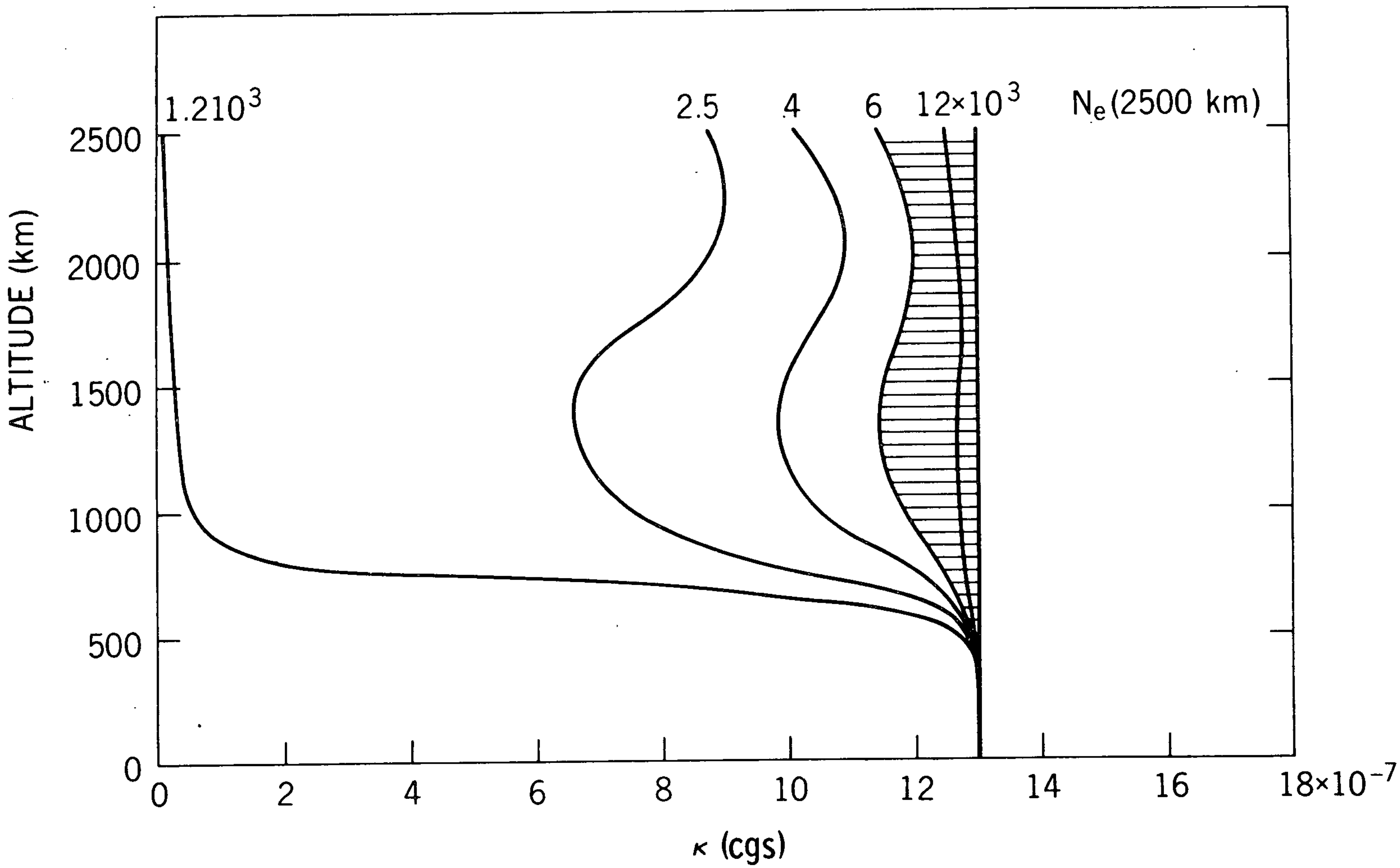

Figure 2. Calculated effective heat conductivity for different density profiles.

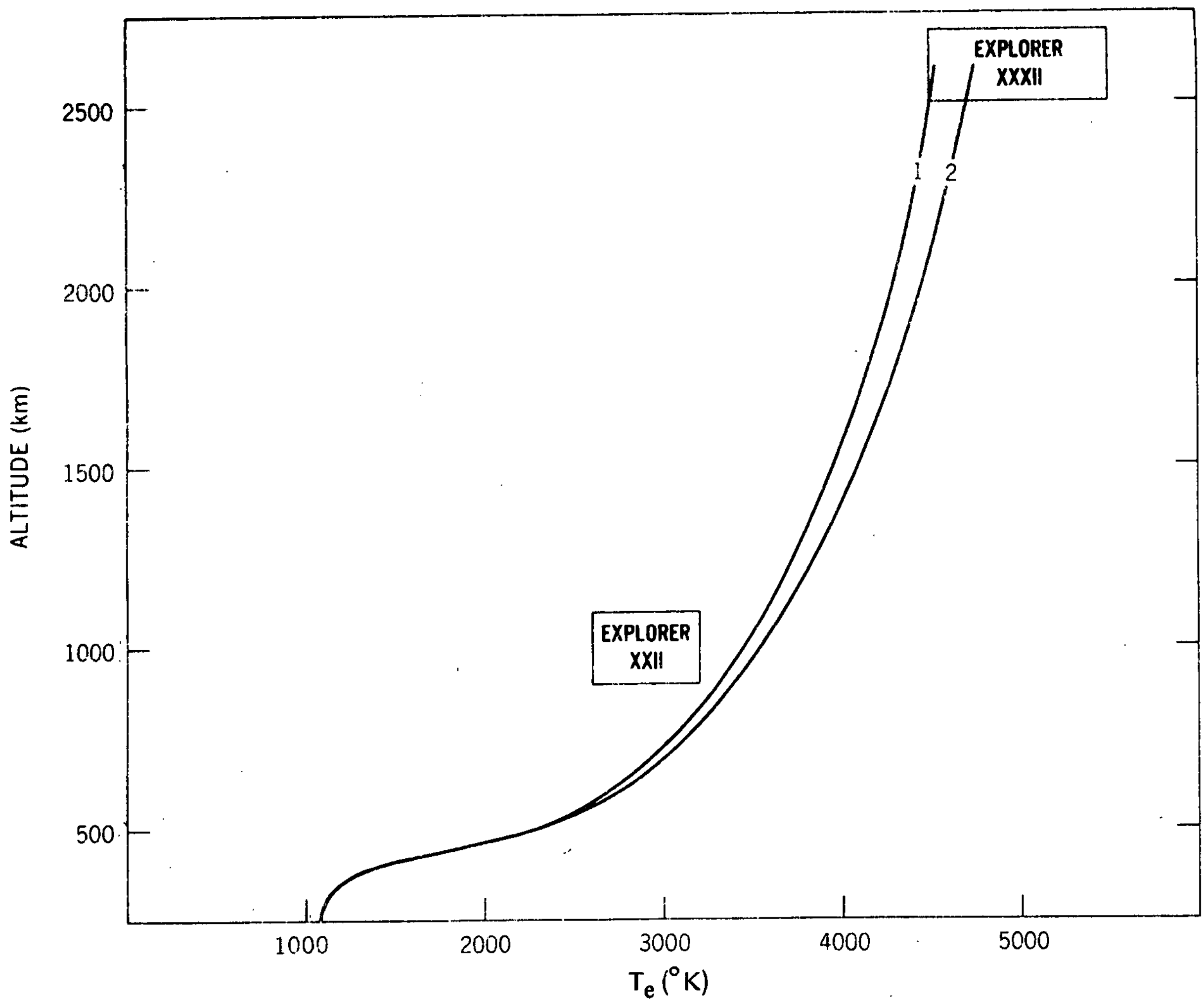

Figure 3. Calculated temperature profiles for the cases of the conductivities κ_{SH} (curve 1) and κ_{eff} (curve 2).

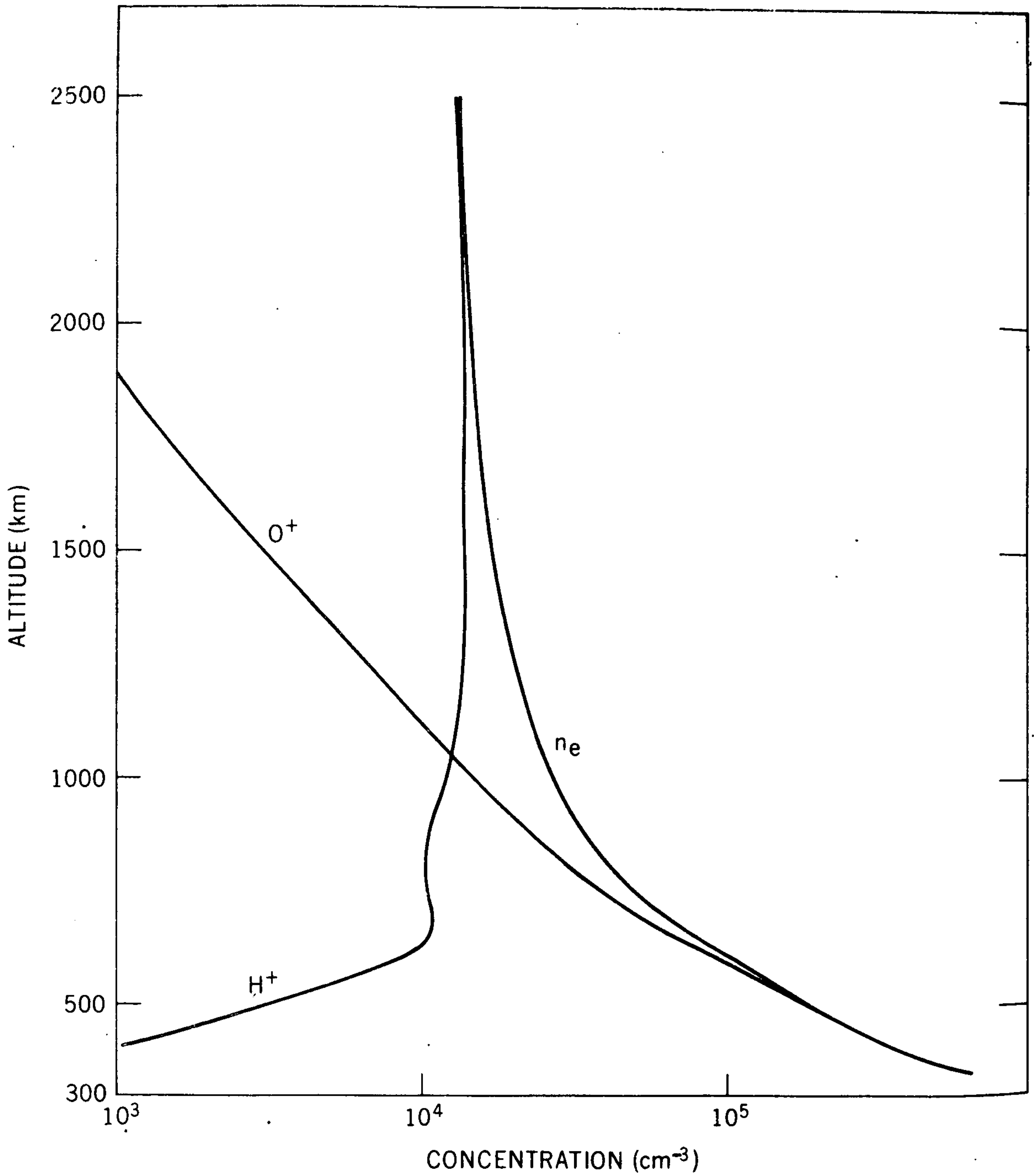

Figure 4. O^+, H^+, and electron density profiles corresponding to the temperature profile of curve 2 in Figure 3.

NASA–GSFC